ELSEVIER

Physica E 10 (2001) 576–586

PHYSICA E

www.elsevier.nl/locate/physe

Interband tunneling depopulation in type-II InAs/GaSb cascade laser heterostructure

Mikhail V. Kisin[a,*], Michael A. Stroscio[b], Serge Luryi[a], Gregory Belenky[a]

[a]*Department of Electrical and Computer Engineering, State University of New York at Stony Brook, NY 11794-2350, USA*
[b]*US Army Research Office, P.O. Box 12211, Research Triangle Park, NC 27709-2211, USA*

Received 22 September 2000; accepted 5 December 2000

Abstract

An exact analytical representation has been obtained for electron eigenstates in the full isotropic 8-band Kane model and applied to calculate the depopulation rate of the lower lasing state in the active region of a type-II intersubband cascade laser. We show that interband tunneling rate takes its maximum value when the depopulated states belong to the upper of the coupled electron- and hole-like subbands in the "leaky window" of the broken-gap InAs/GaSb heterostructure.
© 2001 Elsevier Science B.V. All rights reserved.

PACS: 73.23.−b; 73.40.Gk; 73.61.Ey

Keywords: Type-II semiconductor heterostructures; Interband tunneling; Cascade laser

1. Introduction

Recently, mid-infrared interband quantum cascade lasers (QCL) based on type-II semiconductor heterostructures [1] were demonstrated with output optical characteristics at $\lambda \approx 3.5$ μm [2,3] comparable to the best of type-I QCL [4]. For long-wavelength applications beyond 5 μm the intersubband cascade design, successfully implemented in InGaAs/InAlAs QCL [5], is especially promising. The intersubband lasing scheme can be realized also in GaSb-based type-II cascade heterostructures [6], where the main advantage over type-I heterostructures is the more effective depopulation of the lower lasing subband owing to the high rate of interband tunneling process through the "leaky window" (overlap of the InAs conduction and GaSb valence bands) [7,8]. The theory of the interband tunneling in type-II heterostructures must include accurately the band-mixing effect, since the electron states of both conduction and valence bands of the constituent semiconductors participate in the tunneling process on equal footing. Direct numerical solution of the matrix multiband

* Corresponding author. Tel.: +1-516-632-8421; fax: +1-516-632-8494.
E-mail address: mvk@ece.sunysb.edu (M.V. Kisin).

1386-9477/01/$ - see front matter © 2001 Elsevier Science B.V. All rights reserved.
PII: S1386-9477(01)00151-5

Schrödinger equation, most commonly employed for this task [9], is numerically costly and cannot provide a clear physical picture of the process. For symmetrical leaky quantum wells, an illustrative analytical approach to the interband tunneling was developed earlier in the framework of a simplified two-band model [10]. In the current work, we show that even for asymmetrical type-II cascade structures an analytical description of the interband tunneling process in the framework of the full isotropic eight-band Kane model is quite possible, which is especially valuable for application to laser design. We obtain exact solutions for both "light" and "heavy" eigenstates in narrow-gap semiconductor energy spectrum. As an application of our approach, we consider the depopulation of the lowest lasing level in a model three-layer InAs/GaSb/InAs heterostructure shown in Fig. 1. The utmost left infinite barrier region models an AlSb layer, layers A and B represent InAs/GaSb double-quantum-well active region, and the adjacent half-space of the InAs models the collector/emittor region of a type-II cascade intersubband laser. The position ε and the width Γ of the quasibound states in the leaky window δ are inferred from the peaks of the reflection coefficient phase derivative with respect to energy. Our calculations confirm that heavy resonant states, neglected in previous approaches, do not participate noticeably in the interband tunneling process. We show that the rate of the interband tunneling through the light quasiparticle states takes its maximum value when the depopulated states in the laser active region belong to the upper of the coupled electron- and light-hole-like subbands in the leaky window of the type-II heterostructure.

2. The model

An accurate model of the interband tunneling in narrow-gap type-II heterostructures should be based on a multiband description of the electron dynamics explicitly taking into account all the states participating in the tunneling process. In what follows, we shall use the full 8-band Kane model in the representation given by four Kramers-conjugate pairs of coupled spin $\{\alpha,\beta\}$ and orbital $\{S,X,Y,Z\}$ basis states:

$$\{u_n^v\} = \left\{ \begin{pmatrix} S\alpha \\ S\beta \end{pmatrix}, \frac{1}{\sqrt{6}} \begin{pmatrix} 2Z\alpha - (X+\mathrm{i}Y)\beta \\ 2Z\beta + (X-\mathrm{i}Y)\alpha \end{pmatrix}, \frac{1}{\sqrt{3}} \begin{pmatrix} Z\alpha + (X+\mathrm{i}Y)\beta \\ Z\beta - (X-\mathrm{i}Y)\alpha \end{pmatrix}, \frac{1}{\sqrt{2}} \begin{pmatrix} (X+\mathrm{i}Y)\alpha \\ (X-\mathrm{i}Y)\beta \end{pmatrix} \right\},$$

$$n = 0,1,2,3, \quad v = \pm 1. \tag{1}$$

2.1. The Hamiltonian

Assuming isotropic energy spectra in the bulk constituent semiconductors, we can write the 8-band Kane Hamiltonian in the form,

$$\hat{H} = E_\mathrm{g}\hat{B}_1 + \Delta\frac{\hat{\mathbf{J}}\cdot\hat{\boldsymbol{\sigma}} - 1}{3}\hat{B}_3 + \hat{\mathbf{P}}\cdot\mathbf{p} + \gamma_1 p^2\hat{B}_1 - \gamma_3 p^2\hat{B}_3 - \frac{1}{2}\gamma_2(\mathbf{p}\cdot\hat{\mathbf{J}})(\mathbf{p}\cdot(\hat{\mathbf{J}}+\hat{\boldsymbol{\sigma}})). \tag{2}$$

Here $\mathbf{p} = -\mathrm{i}\nabla$ is the momentum operator, and we employ the unit system with $\hbar = 1$. Symbols with hats represent square 8×8 matrices. The matrices $\hat{B}_1$ and $\hat{B}_3$ are diagonal unit matrices in the scalar $(n=0)$ and the vector $(n=1,2,3)$ subspaces, expressing the intraband nature of related operators, while the nondiagonal matrix operator $\hat{\mathbf{P}}$ corresponds to the interband kp-mixing, characterized by Kane's velocity, $P = 1/m_0\langle S|\partial/\partial z|Z\rangle$. Phenomenological coefficients γ_i in the second-order terms can easily be related to the experimentally determined effective masses (cf. the appendix).

The second term of the Hamiltonian, also denoted by $\hat{H}_\mathrm{so}$, describes the spin–orbit splitting of the vector subspace basis states by the amount Δ due to coupling between the microscopic angular momenta $\mathbf{J}=1$ and $\frac{1}{2}\boldsymbol{\sigma}$. In the vector subspace within the basis of coupled angular momenta (1) the matrix $\mathbf{J}\cdot\boldsymbol{\sigma}$ becomes

diagonal

$$\mathbf{J}\cdot\boldsymbol{\sigma} = \begin{bmatrix} 1 & 0 & 0 \\ 0 & -2 & 0 \\ 0 & 0 & 1 \end{bmatrix} \delta_{\nu\nu'}. \tag{3}$$

Hence the operator $\hat{H}_{so}$ has nonzero matrix elements only for $n = 2$; in this case

$$(H_{so})_{22}^{(1)} = (H_{so})_{22}^{(-1)} = -\Delta, \tag{4}$$

assuming that the highest energy level in the valence band corresponds to the four-fold degenerate basis states with $n = 1, 3$.

The matrix structure of the last second-order term in Eq. (2) relates to the quasispin operator $\hat{\boldsymbol{\Sigma}} = \hat{\mathbf{J}} + \frac{1}{2}\hat{\boldsymbol{\sigma}}$. This operator satisfies the usual commutation rule, $\hat{\boldsymbol{\Sigma}} \times \hat{\boldsymbol{\Sigma}} = \mathrm{i}\hat{\boldsymbol{\Sigma}}$, and guarantees the conservation of the effective angular momentum $\hat{\boldsymbol{\Sigma}} + \hat{\mathbf{L}}$, defined in the space of 8-component envelopes:

$$\lfloor \hat{H}, (\hat{\boldsymbol{\Sigma}} + \hat{\mathbf{L}}) \rfloor = 0, \quad \hat{\mathbf{L}} = \mathbf{r} \times \mathbf{p}. \tag{5}$$

Since the helicity of a free quasiparticle with momentum $\mathbf{k}$, $\hat{\mu} = (\mathbf{k}\cdot\hat{\boldsymbol{\Sigma}})/k$, is a good quantum number, the scalar invariant $(\mathbf{p}\cdot\hat{\boldsymbol{\Sigma}})^2$ is admissible in the Hamiltonian. In Eq. (2), we use the more convenient matrix form, $(\mathbf{p}\cdot\hat{\boldsymbol{\Sigma}})^2 - p^2/4 = (\mathbf{p}\cdot\hat{\mathbf{J}})(\mathbf{p}\cdot(\hat{\mathbf{J}} + \hat{\boldsymbol{\sigma}}))$, which is directly related to the projection operator onto the subspace of heavy eigenstates

$$\hat{\Lambda}_h = \frac{1}{2}\left(\hat{\mu}^2 - \frac{1}{4}\right) = \frac{1}{2k^2}(\mathbf{k}\cdot\hat{\mathbf{J}})(\mathbf{k}\cdot(\hat{\mathbf{J}} + \hat{\boldsymbol{\sigma}})). \tag{6}$$

This operator annuls the wave functions with helicity $\mu = 1/2$ and, therefore, can be considered as a projection operator onto the subspace of two-fold degenerate ($\mathrm{Sp}\,\hat{\Lambda}_h = 2$) heavy eigenstates, characterized by the helicity $\mu = 3/2$ and the dispersion

$$E_h(k) = \tfrac{1}{2}\mathrm{Sp}(\hat{\Lambda}_h \hat{H}) = -(\gamma_2 + \gamma_3)k^2. \tag{7}$$

2.2. *The eigenfunctions*

The projection operator Λ_h facilitates obtaining an analytical expression for the heavy eigenstates

$$\Psi_h = \hat{\Lambda}_h \begin{pmatrix} 1 \\ \mathbf{V} \end{pmatrix} = \begin{pmatrix} 0 \\ \mathbf{V}_h \end{pmatrix} V_{h0}, \quad \mathbf{V}_h \propto \mathbf{V} - [(\mathbf{k}\cdot\mathbf{V})\mathbf{k} - \mathrm{i}(\mathbf{k}\cdot\boldsymbol{\sigma})\mathbf{k}\times\mathbf{V}]/k^2. \tag{8}$$

In the latter relation, the expression of the vector multiplication operation through the matrices J of angular momentum 1 is used, $\mathbf{k}\times\mathbf{V} = -\mathrm{i}(\mathbf{k}\cdot\mathbf{J})\mathbf{V}$, in analogy with the Majorana representation of Maxwell's equations [11]. V_{h0} is a normalizing spinor, which includes also the spatial dependence $V_{h0} \propto \exp(\mathrm{i}\mathbf{k}r)$. In the basis of the coupled angular momenta, the corresponding representation is

$$\Lambda_h = \frac{1}{2k^2}\begin{bmatrix} \frac{3}{2}k_\parallel^2 & 0 & -\frac{\mathrm{i}\sqrt{3}}{2}(\mathbf{k}\cdot\boldsymbol{\sigma} + k_z\sigma_z)\sigma_y(\mathbf{k}_\parallel\cdot\boldsymbol{\sigma}_\parallel) \\ 0 & 0 & 0 \\ \frac{\mathrm{i}\sqrt{3}}{2}(\mathbf{k}_\parallel\cdot\boldsymbol{\sigma}_\parallel)\sigma_y(\mathbf{k}\cdot\boldsymbol{\sigma} + k_z\sigma_z) & 0 & \frac{1}{2}(k^2 + 3k_z^2) \end{bmatrix}, \tag{9}$$

$$\mathbf{V}_\mathrm{h} \propto \Lambda_\mathrm{h} \begin{pmatrix} 1 \\ 0 \\ 0 \end{pmatrix} \propto \begin{pmatrix} \sqrt{3}k_\parallel^2 \\ 0 \\ \mathrm{i}(\mathbf{k}_\parallel \cdot \boldsymbol{\sigma}_\parallel)\sigma_y(\mathbf{k}\cdot\boldsymbol{\sigma} + k_z\sigma_z) \end{pmatrix}, \quad k_\parallel^2 = k_x^2 + k_y^2. \tag{10}$$

For light eigenstates the vector part of the wave function, $\mathbf{V}_\mathrm{l}$, is determined by the interband coupling term $\hat{\mathbf{P}} \cdot \mathbf{p}$ in the Hamiltonian and thus should be linear in quasiparticle wave vector $\mathbf{k}$. In Kane's model, both independent Hermitian operators, $\mathbf{p}$ and $\mathbf{p} \times \boldsymbol{\sigma}$, exhibit the transformation properties of a polar vector, therefore, $\mathbf{V}_\mathrm{l}$ should be sought as a linear combination of the column $\mathbf{k}$ and the column $\mathbf{q} = \boldsymbol{\sigma} \times \mathbf{k} = -\mathrm{i}(\boldsymbol{\sigma} \cdot \mathbf{J})\mathbf{k}$:

$$\Psi_\mathrm{l} = \begin{pmatrix} 1 \\ \mathbf{V}_\mathrm{l} \end{pmatrix} V_{\mathrm{l}0}, \quad \mathbf{V}_\mathrm{l} = \mathrm{i}P(a + b(\boldsymbol{\sigma}\cdot\mathbf{J}))\mathbf{k}. \tag{11}$$

Substituting (11) into the Schrödinger equation, $\hat{H}\Psi_\mathrm{l} = E\Psi_\mathrm{l}$, and making use of the relation $\hat{\Lambda}_\mathrm{h}\Psi_\mathrm{l} \equiv 0$, we easily obtain the coefficients of the linear combination:

$$a = \frac{\tilde{E} + \frac{2}{3}\Delta}{\tilde{E}(\tilde{E}+\Delta)}, \quad b = \frac{\frac{1}{3}\Delta}{\tilde{E}(\tilde{E}+\Delta)}, \quad \tilde{E} = E + \gamma_3 k^2. \tag{12}$$

Vector column $\mathbf{V}_\mathrm{l}$ takes an especially simple form in the coupled momenta basis due to the diagonal representation of the spin–orbit coupling (3):

$$V_\mathrm{l} = \begin{bmatrix} \frac{1}{\tilde{E}} & 0 & 0 \\ 0 & \frac{1}{\tilde{E}+\Delta} & 0 \\ 0 & 0 & \frac{1}{\tilde{E}} \end{bmatrix} \mathrm{i}P\mathbf{k}\delta_{vv'}, \quad \mathbf{k} = \begin{pmatrix} (2k_z + \mathrm{i}q_z)/\sqrt{6} \\ (k_z - \mathrm{i}q_z)/\sqrt{3} \\ (-q_z\sigma_y)/\sqrt{2} \end{pmatrix}. \tag{13}$$

The dispersion relation for the corresponding light bands can be obtained in a similar fashion to Eq. (7) and it is of third-order in k^2

$$\det\{(1 - \hat{\Lambda}_\mathrm{h})(\hat{H} - E)\} = (E_\mathrm{g} + \gamma_1 k^2 - E) + P^2k^2 \frac{\tilde{E} + \frac{2}{3}\Delta}{\tilde{E}(\tilde{E}+\Delta)} = 0. \tag{14}$$

Thus, in the eight-band Kane model there are three different types of light eigenstates (cf. Eq. (11)). Usually, we have $\gamma_1, \gamma_3 \ll P^2/E_\mathrm{g}$, and only two functions, Ψ_{11} and Ψ_{12}, are physically relevant. These functions describe, respectively, the conduction/light-hole and the spin–orbit split-off bands.

Next, we can significantly simplify the problem by taking into account the reflection symmetry in the plane formed by the unit vector $\mathbf{n}_z$ normal to the interfaces and the two-dimensional wave vector $\mathbf{K}$ chosen along the x-axis. This transformation can be represented as a product of the inversion, $\hat{I}$, and the rotation by π about the y-axis. In the basis (1) it corresponds to the matrix

$$\hat{\omega}_{xz} = \exp(\mathrm{i}\pi\hat{\Sigma}_y)\hat{I} = (\hat{B}_1 + \hat{B}_3) \otimes \mathrm{i}\sigma_y. \tag{15}$$

We choose the normalizing spinors $V_{\mathrm{l}0}$ and $V_{\mathrm{h}0}$ as eigenstates of the operator σ_y:

$$\sigma_y V_0 = \omega V_0, \tag{16}$$

thus introducing in our model the parity of the state, $\omega = \pm 1$.[1] Solutions (10) and (13) then reduce to

$$\mathbf{V}_{\rm h} = \begin{pmatrix} \sqrt{3}K \\ 0 \\ -(2k_z + {\rm i}\omega K) \end{pmatrix}, \quad \mathbf{V}_{\rm l} = {\rm i}P \begin{pmatrix} (2k_z - {\rm i}\omega K)/\sqrt{6}\tilde{E} \\ (k_z + {\rm i}\omega K)/\sqrt{3}(\tilde{E} + \Delta) \\ K/\sqrt{2}\tilde{E} \end{pmatrix}. \tag{17}$$

2.3. Boundary conditions

At the heterointerface, we impose boundary conditions [12] that generalize the usual EFA approach:

$$\psi_{n\rm A} = F_n \psi_{n\rm B}, \quad \psi'_{n\rm A} = G_n \psi'_{n\rm B}. \tag{18}$$

Matching parameters F_n and G_n are related to the Hamiltonian parameters of the constituent semiconductors due to the current continuity across the interface. In bulk semiconductors the current density satisfies the continuity equation

$$\operatorname{div} \mathbf{j} = -\frac{\partial \Psi^+ \Psi}{\partial t} = {\rm i}(\Psi^+ \hat{H} \Psi - (\hat{H}\Psi)^+ \Psi). \tag{19}$$

In model (2) this equation is satisfied by the expression

$$\begin{aligned} \mathbf{j} = {} & \Psi^+ \hat{\mathbf{P}} \Psi + (\gamma_1 \hat{B}_1 - \gamma_3 \hat{B}_3)(\Psi^+ \mathbf{p} \Psi + {\rm h.c.}) \\ & - \frac{1}{2}\gamma_2 \left[\left(\Psi^+ \left(\hat{\mathbf{J}}(\mathbf{p}\cdot\hat{\mathbf{J}}) + \frac{\hat{\boldsymbol{\sigma}}(\mathbf{p}\cdot\hat{\mathbf{J}}) + \hat{\mathbf{J}}(\mathbf{p}\cdot\hat{\boldsymbol{\sigma}})}{2} \right) \Psi + {\rm h.c.} \right) \right] \end{aligned} \tag{20}$$

with the z-component represented in basis (1) as

$$\begin{aligned} j_z = {} & -{\rm i}P[\psi_0^* (\sqrt{\tfrac{2}{3}}\psi_1 + \sqrt{\tfrac{1}{3}}\psi_2) - {\rm c.c.}] - {\rm i}\gamma_1(\psi_0^* \psi_0' - {\rm c.c.}) + {\rm i}\gamma_3(\psi_1^* \psi_1' + \psi_2^* \psi_2' - {\rm c.c.}) \\ & + {\rm i}(\gamma_2 + \gamma_3)(\psi_3^* \psi_3' - {\rm c.c.}) - \tfrac{\sqrt{3}}{2}\gamma_2[\psi_3^*(p_x - {\rm i}\sigma_x p_y)\psi_1 + {\rm c.c.}]. \end{aligned} \tag{21}$$

For an arbitrary mesoscopic state Ψ, all of the wave function components ψ_n can be treated independently, so the continuity of the z-component of the current, $j_{z\rm A} = j_{z\rm B}$, entails the following relationship between the matching parameters F_n, G_n and the Hamiltonian parameters:

$$F_0 F_1 = F_0 F_2 = \frac{P_{\rm B}}{P_{\rm A}}, \quad F_1 F_3 = \frac{\gamma_{2\rm B}}{\gamma_{2\rm A}}, \tag{22a}$$

$$F_0 G_0 = \frac{\gamma_{1\rm B}}{\gamma_{1\rm A}}, \quad F_1 G_1 = F_2 G_2 = \frac{\gamma_{3\rm B}}{\gamma_{3\rm A}}, \quad F_3 G_3 = \frac{(\gamma_2 + \gamma_3)_{\rm B}}{(\gamma_2 + \gamma_3)_{\rm A}}. \tag{22b}$$

3. Dispersion equation for a "leaky" double quantum well

Analytical expression (17) for the eigenstates of the 8-band Kane model is the key to further analysis of the energy spectrum in type-II laser heterostructures. As a next approximation, we can use the limit of large spin–orbit splitting of the valence band, $\Delta \gg E$, which is a hallmark of the narrow-gap semiconductors InAs

[1] The parity ω correlates also with the sign of the state polarization in y-direction because of the commutativity of corresponding operators, $[\hat{\Sigma}_y, \hat{\omega}_{xz}]_- = 0$.

and GaSb. In this limit, an arbitrary mesoscopic state is represented in each layer by a superposition of smooth wave packets of only one light and one heavy solution (17), where the components with $n=2$ can be omitted

$$\Psi \approx \Psi_{\rm l} + \Psi_{\rm h} = \begin{pmatrix} \psi_0 \\ \psi_1 \\ \psi_3 \end{pmatrix}. \tag{23}$$

The matching conditions are significantly simplified also. For the effective wave function derivatives at the interface, we can write schematically, dropping the index z,

$$(k_{\rm h}\Psi_{\rm h} + k_{\rm l}\Psi_{\rm l})_{\rm A} \propto G(k_{\rm h}\Psi_{\rm h} + k_{\rm l}\Psi_{\rm l})_{\rm B}. \tag{24}$$

In the InAs layers, where the energy of the state significantly exceeds the valence band maximum, we have $|k_{\rm h}| \gg k_{\rm l}$. Assuming all terms in Eq. (24) to be of the same order of magnitude, the heavy component of the effective wave function (23) in material A is estimated as

$$\Psi_{\rm h}^{\rm A} \propto \frac{k_{\rm l}^{\rm A}}{k_{\rm h}^{\rm A}} \Psi_{\rm l}^{\rm A} \ll \Psi_{\rm l}^{\rm A}. \tag{25}$$

On these grounds, small amplitudes $\Psi_{\rm h}$ in both A-layers (InAs) can be neglected, so that the boundary conditions for the smooth part of the effective wave function are represented only by the relations (22a).

In the flat-band approximation, the wave function of an electron state in each layer is a superposition of partial solutions with opposite k_z: $\Psi_{\rm l,h}^{\pm} = U_{\rm l,h}^{\pm}\Psi_{\rm l,h}(\pm k_z)$. In the left half-space (barrier region) the light solution is purely evanescent with dominant component $\psi_{11} \gg \psi_{10}, \psi_{13}$, hence at the boundary $\psi_0 = \psi_3 = 0$. In the right half-space layer of InAs we assume the amplitude of the incoming wave $U_{\rm l}^{+} = 0$, so that only the outgoing wave $\Psi_{\rm l}^{-}$ is present there. After some notorious but straightforward algebra the boundary condition problem results in the following dispersion equation:

$$\begin{aligned} D(\varepsilon) = {} & \sin(k_{\rm lA}d_{\rm A})\sin(k_{\rm lB}d_{\rm B})\sin(k_{\rm hB}d_{\rm B})\left\{ \left(k_{\rm hB}^2 + \frac{1}{4}K^2\right) \right. \\ & \times \left[k_{\rm lB}^2 + \frac{1}{4}K^2 - \xi\left(\xi\lambda_1\lambda_2 + (\lambda_1+\lambda_2)k_{\rm lB}\cot k_{\rm lB}d_{\rm B} + \frac{1}{4}K^2(2-\xi) + \frac{\omega K}{2}\xi(1-\xi)(\lambda_1-\lambda_2)\right)\right] \\ & + \frac{3}{4}K^2\left(1-\tilde{\xi}\right)\left[2k_{\rm lB}k_{\rm hB}\frac{1-\cos k_{\rm lB}d_{\rm B}\cos k_{\rm hB}d_{\rm B}}{\sin k_{\rm lB}d_{\rm B}\sin k_{\rm hB}d_{\rm B}} - \xi k_{\rm hB}\cot k_{\rm hB}d_{\rm B}(\lambda_1+\lambda_2) - \frac{\omega K}{2}\xi(\lambda_1-\lambda_2)\right] \\ & \left. + \frac{3}{16}K^4(1-\tilde{\xi})[2(1-\xi)+3(1-\tilde{\xi})]\right\} = 0. \end{aligned} \tag{26}$$

Here,

$$\lambda_1 = k_{\rm lA}\cot k_{\rm lA}d_{\rm A}, \quad \lambda_2 = -{\rm i}k_{\rm lA}, \quad \xi = \frac{E_{\rm B}}{E_{\rm A}F_1^2}, \quad \tilde{\xi} = \frac{E_{\rm B}}{E_{\rm A}}\frac{\gamma_{2\rm A}}{\gamma_{2\rm B}},$$

$$k_{\rm lA,B}^2 + K^2 = E_{\rm A,B}(E_{\rm A,B} - E_{\rm GA,B})/\tfrac{2}{3}P_{\rm A,B}^2, \quad k_{\rm hB}^2 + K^2 = -E_{\rm B}/(\gamma_2+\gamma_3)_{\rm B}. \tag{27}$$

The energy E in each layer is referenced to the top of the valence band, so that

$$E_{\rm A} = E_{\rm GA} + \varepsilon = E_{\rm B} + E_{\rm GA} + \delta,$$

where ε is the energy of the level in the leaky window δ counted from the InAs conduction band minimum. In the equations above, $E_{\rm GA}$ and $E_{\rm GB}$ refer to energy gaps of the constituent semiconductors. It is interesting that only one boundary condition set, (22a), determines the dispersion equation. The second set of boundary conditions, (22b), would come into play if the valence band discontinuity were not so large, so that $|k_{\rm hA}| \approx k_{\rm hB}$ and the heavy states were fully engaged in the tunneling process. In this situation, we would have to use the

matching condition for derivatives (24) to determine the amplitudes Ψ_h in the A-layers. In the heterostructure under study, the B-type heavy states of the GaSb quantum well still participate in the process, but only because of the "light"–"heavy" mixing at the InAs/GaSb interface occurring at final K due to the final values of the third component of $\mathbf{V}_l$ and the first component of $\mathbf{V}_h$ in Eq. (17).

4. Results and discussion

The dispersion equation (26) contains complete information about energy levels and subband dispersions in both electron- and hole-like subbands in the model type-II heterostructure shown in Fig. 1. Terms with ω describe spin splitting of the subbands induced by the spin–orbital interaction in an asymmetric system. The imaginary term λ_2 corresponds to the outgoing electron wave in the right half-space layer of InAs. This makes the energy eigenvalues E complex with imaginary part $-i\Gamma/2$ representing the final lifetime of the quasibound electron energy levels. For the lower lasing state E_A in the left InAs quantum well A this corresponds to interband tunneling through the adjacent hole quantum well B (GaSb layer).

For the electron states close to the subband bottoms, some valuable information can be obtained analytically. At $K=0$, the heavy particle states are completely decoupled from the light states and the dispersion equation for the latter reveals a very simple form convenient for further analytical treatment

$$\sin k_A d_A \sin k_B d_B = \xi_0 [\cos k_A d_A \cos k_B d_B - i(\xi_0 \cos k_A d_A \sin k_B d_B + \sin k_A d_A \cos k_B d_B)] \tag{28}$$

where

$$\xi_0 = \xi \frac{k_A}{k_B}$$

and index l is omitted for simplicity. To estimate the level widths, $\Gamma_{A,B}$, we can use the limiting case of a parabolic spectrum: $k_A^2 = 2m_A\varepsilon$, $k_B^2 = 2m_B(\delta - \varepsilon)$, $\delta \ll E_{GA,B}$. This entails

$$\xi_0^2 = \frac{F_0^2}{F_1^2} \frac{\varepsilon(\delta - \varepsilon)}{E_{GA}E_{GB}} \ll 1. \tag{29}$$

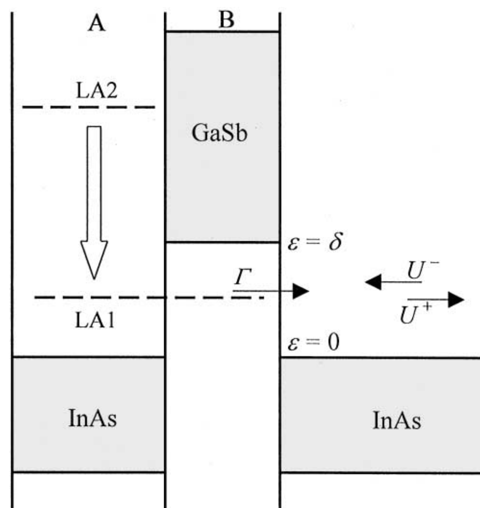

Fig. 1. Schematic band diagram of a "leaky" double quantum well heterostructure.

In this approximation the dispersion equation (28) can easily be split into real and imaginary parts and, assuming $\Gamma \propto \xi_0$, we arrive at the relations

$$\tan k_A d_A \tan k_B d_B \cong \xi_0, \tag{30}$$

$$\Gamma \cong \frac{2\xi_0}{d_A\sqrt{m_A/2\varepsilon}\tan k_B d_B/\tan k_A d_A - d_B\sqrt{m_B/2(\delta-\varepsilon)}}. \tag{31}$$

For the lowest electron-like level localized mainly in the InAs quantum well, one has $k_A \propto \pi/d_A$, and $\tan k_A d_A \propto \xi_0 \ll 1$, whereas for the upper hole-like light level in the GaSb layer, we likewise have $k_B \propto \pi/d_B$, and $\tan k_B d_B \propto \xi_0$. As a result, from Eq. (31) we obtain the estimations

$$\Gamma_A \approx \frac{4\varepsilon}{\pi}\xi_0^2 \cot^2 k_B d_B, \quad \Gamma_B \approx \frac{4(\delta-\varepsilon)}{\pi}\xi_0. \tag{32}$$

When A- and B-type levels anticross, the level widths, $\Gamma_{A,B}$, should be equal, because the electron state is equally distributed between both coupled quantum wells. Beyond the anticrossing, the quasibound A-states are substantially narrower than the B-states, $\Gamma_A \propto \xi_0^2 \ll \Gamma_B \propto \xi_0$, since the depopulation of an A-level via interband tunneling requires two interfaces to penetrate. We can trace this situation by accurate numerical solution of the dispersion equation (28). The results are presented in Fig. 2, which shows the position and width of the

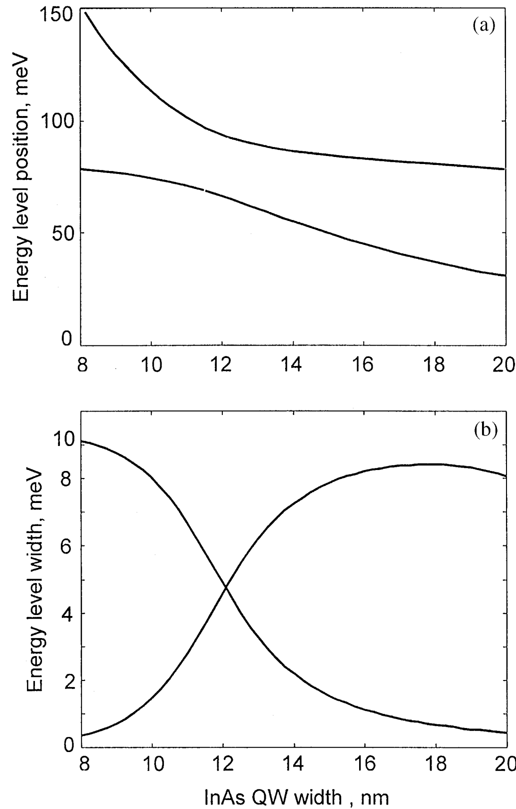

Fig. 2. Position (a) and energy width (b) of the lowest electron and the highest light-hole energy levels at $K = 0$ as a function of the InAs quantum well width d_A. The width of GaSb quantum well is $d_B = 10$ nm. Other parameters used are: $\delta = 150$ meV, $E_G^{InAs} = 400$ meV, $E_G^{GaSb} = 800$ meV, $F_1 = 1$.

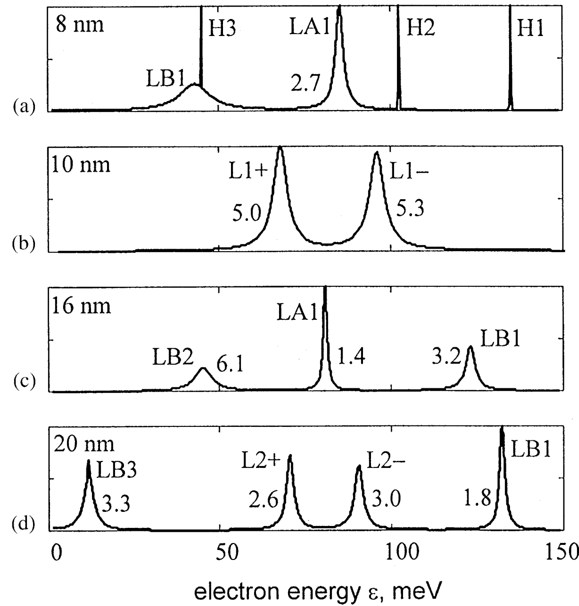

Fig. 3. Derivative of the phase of the reflection coefficient with respect to energy as a function of the energy ε in the leaky window δ. The curves are normalized to the highest L-type peak and labeled with the full peak width at half maximum Γ. Each subplot is labeled with the GaSb layer width d_B in nanometers. The width of the InAs quantum well is $d_A = 10$ nm.

energy levels $\varepsilon_{A,B}$ as a function of the InAs quantum well width, d_A. The energy level widths coincide at the anticrossing point where the depopulation rate, Γ_A, for the lower lasing state in the intersubband design scheme is readily the highest.

At arbitrary K, the positions and the widths of the quasibound states in the leaky window δ can be inferred from the peaks of the reflection coefficient phase derivative with respect to energy [13]. Restoring the amplitude of the incoming wave, U_1^-, in the right half-space layer of InAs, we obtain the reflection coefficient in the form

$$R(\varepsilon) = \left(\frac{U_1^+}{U_1^-}\right) = \frac{D^*(\varepsilon)}{D(\varepsilon)}. \tag{33}$$

Since there is no propagating wave in the left barrier region, the latter relation readily follows also from the time-reversal symmetry of the reflection process. In the vicinity of a resonant state the reflection coefficient will undergo π phase shift with the peak of the phase derivative with respect to energy having Lorentzian shape. The value of the full peak width at half maximum represents the inverse lifetime Γ of the quasibound state.

Figs. 3a–d, labeled with the GaSb quantum well width d_B in nm, show the evolution of the resonant states in the energy range $0 < \varepsilon < \delta$ as d_B increases. The InAs layer width is kept constant, $d_A = 12$ nm. Three narrow peaks, H1, H2 and H3, with $\Gamma = 0.12$, 0.15 and 0.01 meV, respectively, correspond to heavy quasibound states, which appear only for nonzero values of the 2D wave vector K. In Fig. 3a we take $K = 0.025\ \text{nm}^{-1}$, for all other subplots $K = 0$. Peak LA1 with $\Gamma = 2.7$ meV corresponds to the lowest electron-like subband localized mostly in InAs quantum well A. Peak LB1 with $\Gamma = 10.7$ meV corresponds to the highest light-hole subband of GaSb quantum well B. It is seen readily that narrow heavy quasibound states do not participate noticeably in the interband tunneling depopulation process, which is associated primarily with the decay of light quasibound states, either electron-like, LA, or hole-like, LB. When the A- and B-type levels anticross, the

decay rates of the light states become comparable since the electron density spreads equally over both coupled quantum wells. In Fig. 3b peaks L1+ and L1− represent symmetrical and antisymmetrical combinations of A- and B-levels under anticrossing condition. This anticrossing broadening can be traced also in the case of anticrossing between LA1 and the next hole-like level LB2 (see Fig. 3d, peaks L2±). Beyond the anticrossing, in accord with our estimation (32), the quasibound A-type levels are substantially narrower than the B-type levels (see Figs. 3a and c). Fig. 3d demonstrates also the narrowing of the B-levels when they are verging the leaky window edges. This effect can be accounted for by the mismatch in the Bloch structure of the light A- and B-type solutions and agrees well with our approximate analytical expressions for $\Gamma_{A,B}$ (32). Both this approximate expression and results of exact calculations presented in Fig. 3 show that the level alignment of the Fig. 3b gives the highest tunneling depopulation rate. It is important also that, for a GaSb well width of $d_B = 10$ nm (Fig. 3b), the anticrossing gap is $E(\mathrm{L1}-) - E(\mathrm{L1}+) = 28$ meV, which is smaller than the optical phonon energy in InAs, 30 meV. In this case the interband tunneling from the level L1− can be complemented with the efficient optical-phonon/plasmon assisted resonant depopulation process [14,15] through the lower-lying level L1+, thus allowing further increase of the inverse population ratio between the lasing levels LA2 and L1−. Consideration of these processes, however, is beyond the scope of this work and will become subject of our next study.

5. Conclusions

Complex energy eigenvalues of the quasibound electron states in the leaky window of a broken-gap InAs/GaSb heterostructure are analyzed using an exact analytical solution obtained for both the “light” and the “heavy” eigenstates in the framework of the full 8-band Kane model. The position and effective width of the quasibound states are detected from the abrupt variations of the reflection coefficient phase. We demonstrate that this approach enables simple numerical analysis of the depopulation process of the lower lasing states in the active region of intersubband type-II cascade semiconductor laser. Interband tunneling provides a high depopulation rate and is mostly determined by light quasiparticle states in the leaky window. We show that this process can be significantly enhanced and benefits from anticrossing between the lowest electron-like and the highest light-hole-like levels in coupled InAs and GaSb quantum wells.

Acknowledgements

This work was supported by US Army Research Office and grant DAAD190010423.

Appendix

For small k, relations (7) and (14) give the expressions for the electron, light- and heavy hole effective masses, which can be used to relate the phenomenological parameters γ_i with the experimentally determined quantities m_c, m_{lh}, and m_{hh}:

$$\gamma_1 = \frac{1}{2m_c} - \frac{P^2(E_G + \frac{2}{3}\Delta)}{E_G(E_G + \Delta)}, \quad \gamma_3 = \frac{1}{2m_{lh}} - \frac{2}{3}\frac{P^2}{E_G}, \quad \gamma_2 + \gamma_3 = \frac{1}{2m_{hh}}.$$

These equations can also be used to relate the parameters γ_2 and γ_3 with the Luttinger parameters γ_{1L} and $\bar{\gamma}_L$, which describe the light- and heavy-hole masses in the spherical approximation:

$$\gamma_{1L} - 2\bar{\gamma}_L = \frac{m_0}{m_{hh}}, \quad \gamma_{1L} + 2\bar{\gamma}_L = \frac{m_0}{m_{lh}}.$$

References

[1] R.Q. Yang, Microelectron. J. 30 (1999) 1043.
[2] W.W. Bewley, H. Lee, I. Vurgaftman, R.J. Menna, C.L. Felix, R.U. Martinelli, D.W. Stokes, D.Z. Garbuzov, J.R. Meyer, M. Maiorov, J.C. Connolly, A.R. Sugg, G.H. Olsen, Appl. Phys. Lett. 76 (2000) 256.
[3] J.D. Bruno, J.L. Bradshaw, Rui Q. Yang, J.T. Pham, D.E. Wortman, Appl. Phys. Lett. 76 (2000) 3167.
[4] R. Kohler, C. Gmachl, A. Tredicucci, F. Capasso, D.L. Sivco, S.N.G. Chu, A.Y. Cho, Appl. Phys. Lett. 76 (2000) 1092.
[5] C. Gmachl, A. Tredicucci, F. Capasso, A.L. Hutchinson, D.L. Sivco, J.N. Baillargeon, A.Y. Cho, Appl. Phys. Lett. 72 (1998) 3130.
[6] K. Ohtani, H. Ohno, Appl. Phys. Lett. 74 (1999) 1409.
[7] R.Q. Yang, J.M. Xu, Appl. Phys. Lett. 59 (1991) 181.
[8] H. Ohno, L. Esaki, E.E. Mendez, Appl. Phys. Lett. 60 (1992) 3153.
[9] L.R. Ram-Mohan, I. Vurgaftman, J.R. Meyer, Microelectron. J. 30 (1999) 1031.
[10] R.Q. Yang, J.M. Xu, Phys. Rev. B 46 (1992) 6969.
[11] R. Mignani, E. Recami, M. Baldo, Nuovo Cimento 11 (1974) 568.
[12] M. Kisin, B. Gelmont, S. Luryi, Phys. Rev. B 58 (1998) 4605.
[13] E. Anemogiannis, E.N. Glytsis, T.K. Gaylord, Microelectron. J. 30 (1999) 935.
[14] M. Stroscio, M. Kisin, G. Belenky, S. Luryi, Appl. Phys. Lett. 75 (1999) 3258.
[15] M. Kisin, M. Stroscio, G. Belenky, S. Luryi, Appl. Phys. Lett. 73 (1998) 2075.